



# Real time deterministic quantum teleportation over 10 km of single optical fiber channel

HAO ZHAO,<sup>1</sup> JINXIA FENG,<sup>1,2</sup> JINGKE SUN,<sup>1</sup> YUANJI LI,<sup>1,2</sup> AND KUANSHOU ZHANG<sup>1,2,\*</sup>

<sup>1</sup>State Key Laboratory of Quantum Optics and Quantum Optics Devices, Institute of Opto-Electronics, Shanxi University, Taiyuan, Shanxi 030006, China

<sup>2</sup>Collaborative Innovation Center of Extreme Optics, Shanxi University, Taiyuan, Shanxi 030006, China  
\*kuanshou@sxu.edu.cn

**Abstract:** A real time deterministic quantum teleportation over a single fiber channel was implemented experimentally by exploiting the generated EPR entanglement at 1550 nm. A 1342 nm laser beam was used to transfer the classical information in real time and also acted as a synchronous beam to realize the synchronization of the quantum and classical information. The dependence of the fidelity on the transmission distance of the fiber channel was studied experimentally with optimizing the transmission efficiency of the lossy channel that was established to manipulate the beam of the EPR entanglement in Alice's site. The maximum transmission distance of the deterministic quantum teleportation was 10 km with the fidelity of  $0.51 \pm 0.01$ , which is higher than the classical teleportation limit of  $1/2$ . The work provides a feasible scheme to establish metropolitan quantum networks over fiber channels based on deterministic quantum teleportation.

© 2022 Optica Publishing Group under the terms of the [Optica Open Access Publishing Agreement](#)

## 1. Introduction

Quantum entanglement is a fundamental resource for quantum information process. Quantum teleportation exploiting quantum entanglement plays a key role in quantum networks. It can be used in quantum repeaters and quantum computation in long-distance quantum communication networks [1–3]. The entangled states proposed by Einstein, Podolsky, and Rosen were two-particle states quantum-mechanically correlated with respect to their positions and momenta [4]. The Einstein-Podolsky-Rosen (EPR)-entangled states in continuous variable (CV) regime with the quantum correlations between the amplitude and phase quadratures of the optical field was firstly demonstrated by a subthreshold nondegenerate optical parametric amplifier (NOPA) [5]. The 11 dB EPR-entangled states were obtained by coupling two single-mode squeezed states on a 50/50 beam splitter from two degenerate optical parametric amplifier [6]. Quantum teleportation enables the reliable transfer of an unknown quantum state from one location to another. Quantum entanglement was shared by the sender (Alice) and the remote receiver (Bob), which was spatially separated with Alice. Alice distributes the information of an unknown quantum state to Bob through a quantum channel and a classical channel, respectively. Bob can retrieve the unknown quantum state using a basic operation with the information from Alice. During the teleporting process, the original unknown quantum state is not transferred to Bob directly, only its quantum and classical information are sent to Bob.

Quantum teleportation protocol was firstly proposed by Bennett *et al.* in 1993 [7] and implemented experimentally by Bouwmeester *et al.* [8]. Subsequently, theoretical and experimental investigations on quantum teleportation had been reported [9–22]. Up to now, quantum teleportation had been realized utilizing different physical systems, such as discrete variable photonic qubits [9–12], continuous variable (CV) optical modes [13–17], atomic ensemble [18–20], solid-state systems [21,22] and so on. Quantum teleportation over 100 km free-space channels was achieved used entangled photon pairs in 2012 [9]. Recently, a low-Earth orbit

satellite was used to establish a ground-to-satellite uplink channel, quantum teleportation with the transfer distance of 1400 km was implemented, which is the key step towards a global-scale quantum internet [10]. Alternatively, fiber channels are good choice for quantum teleportation across metropolitan quantum networks, which can be highly compatible with the existing classical optical fiber communication system. A 2 km quantum teleportation with photonic qubits based on fiber channels was firstly completed by Marcikic *et al.* in 2003 [11]. Over 100 km fiber channels quantum teleportation with photonic qubits was demonstrated in 2015 [12]. The quantum teleportation over the fiber channel with qubits in discrete variable (DV) systems can be implemented with high fidelity. The maximum transmission distance can reach to the order of 100 km of the optical fiber. However, the probabilistic generation of DV photonic qubits restricts instantaneous quantum teleportation, a time-consuming post-selection processing has to be required in the protocol. It is essential to develop a deterministic quantum teleportation protocol to realize instantaneous transfer of quantum states without post-selection processing in quantum networks and distributed quantum computation. Owing to CV quantum entangled states of light can be generated unconditionally and deterministically, quantum teleportation based on CV optical modes can be achieved to teleport arbitrary unknown quantum states deterministically. The deterministic teleportation of coherent states and quantum states, which based on CV quantum teleportation protocol, was realized in free-space channels in laboratories [13–17]. However, the deterministic quantum teleportation based on fiber channel over dozens of kilometers is essential step towards metropolitan quantum networks, which is also a big challenge because of the attenuation of CV quantum entanglement propagating in optical fiber. The quantum teleportation over the fiber channel with quantum entangled states in CV systems can benefit from deterministic operations and high detection efficiencies, but suffer from intrinsically limited fidelities and transmission distance due to the sensitivity to losses in the fiber channel. CV quantum entanglement distribution over 20 km fiber channel was firstly demonstrated by Feng *et al.* in 2017, which provided a feasible protocol to realize deterministic quantum communication exploiting quantum entanglement at telecommunication wavelength of 1550 nm over optical fiber channel [23]. Subsequently, deterministic quantum teleportation over 6 km fiber channels was completed using CV quantum entangled states at 1342 nm by Huo *et al.* [24], and a dual-channel scheme was used that two beams of EPR entanglement was distributed symmetrically over 3 km of fiber, respectively. In the scheme, the distributed beams of EPR entanglement cannot be manipulated effectively to improve the performance of the CV quantum teleportation like the transmission distance of the fiber channel and the fidelity. For the quantum teleportation, high fidelity and long transfer distance are important indicators, and how to synchronize signals of the classical channel and quantum channel is also important. An active feed-forward was used to realize the synchronization of signals of the classical channel and quantum channel for the quantum teleportation in DV photonic qubits system [9,10]. However, how to realize the synchronization of signals of the classical channel and quantum channel was not involved in the literatures for the quantum teleportation using CV quantum entangled states [13–17,24,25].

In this paper, a deterministic quantum teleportation based on a single-fiber-channel scheme was designed. A lossy channel was established to manipulate the beam of EPR entanglement in Alice's station. The fidelity of the deterministic quantum teleportation was deduced theoretically. The dependences of the fidelity on the transmission distance, excess noise induced by the effect of the depolarized guided acoustic wave Brillouin scattering (GAWBS) in the fiber and the transmission efficiency of the lossy channel were theoretically analyzed. Based on the theoretical analysis, a deterministic quantum teleportation over a single fiber channel was implemented experimentally by exploiting the generated EPR entanglement at 1550 nm. A 1342 nm laser beam was used to transfer the classical information in real time and also acted as a synchronous beam to realize the synchronization of the quantum and classical information. The quantum and classical information were distributed synchronously over a same single mode fiber (SMF), and a

real time deterministic remote quantum teleportation can be realized. The dependence of the fidelity on the transmission distance of the fiber channel was studied experimentally with and without optimizing the transmission efficiency of the lossy channel.

## 2. Theoretical analysis

The scheme of single-channel deterministic quantum teleportation based on a fiber channel is analyzed theoretically. A single NOPA is used to generate EPR-entangled beams, which would be exploited to implement quantum teleportation of a coherent state. The covariance matrix of EPR-entangled beams generated by NOPA is expressed as

$$\sigma = \begin{pmatrix} \langle \delta \hat{X}_a^2 \rangle & 0 & \langle \delta \hat{X}_a \delta \hat{X}_b \rangle & 0 \\ 0 & \langle \delta \hat{Y}_a^2 \rangle & 0 & -\langle \delta \hat{Y}_a \delta \hat{Y}_b \rangle \\ \langle \delta \hat{X}_a \delta \hat{X}_b \rangle & 0 & \langle \delta \hat{X}_b^2 \rangle & 0 \\ 0 & -\langle \delta \hat{Y}_a \delta \hat{Y}_b \rangle & 0 & \langle \delta \hat{Y}_b^2 \rangle \end{pmatrix}, \quad (1)$$

where  $\delta \hat{X}_a$ ,  $\delta \hat{X}_b$  and  $\delta \hat{Y}_a$ ,  $\delta \hat{Y}_b$  are fluctuations of amplitude and phase quadratures of EPR-entangled beams, mode  $a$  and  $b$ , respectively.  $\delta \hat{X}_a^2$ ,  $\delta \hat{X}_b^2$  and  $\delta \hat{Y}_a^2$ ,  $\delta \hat{Y}_b^2$  are fluctuation variances of amplitude and phase quadratures of EPR-entangled beams, mode  $a$  and  $b$ , respectively. If we assume that the fluctuations of amplitude and phase quadratures of the mode  $a$  and  $b$  are identical, respectively, the covariance matrix of EPR-entangled beams can be rewritten as

$$\sigma = \begin{pmatrix} \sigma_a \mathbf{I} & \sigma_{ab} \mathbf{Z} \\ \sigma_{ab} \mathbf{Z} & \sigma_b \mathbf{I} \end{pmatrix}, \quad (2)$$

where  $\mathbf{I} = \begin{pmatrix} 1 & 0 \\ 0 & 1 \end{pmatrix}$ ,  $\mathbf{Z} = \begin{pmatrix} 1 & 0 \\ 0 & -1 \end{pmatrix}$ ,  $\sigma_a = \langle \delta \hat{X}_a^2 \rangle = \langle \delta \hat{Y}_a^2 \rangle$ ,  $\sigma_b = \langle \delta \hat{X}_b^2 \rangle = \langle \delta \hat{Y}_b^2 \rangle$ ,  $\sigma_{ab} = \langle \delta \hat{X}_a \delta \hat{X}_b \rangle = \langle \delta \hat{Y}_a \delta \hat{Y}_b \rangle$ .

In the process of quantum teleportation, Alice holds one beam of EPR-entangled beams (mode  $a$ ). An unknown initial input state is prepared and sent it to Alice. Alice combined the mode  $a$  and an input state on a 50/50 beam splitter (BS) and made a joint measurement. The amplitude and phase quadratures of the output mode from the BS can be obtained as

$$\begin{cases} \hat{X}_u = (\hat{X}_{in} - \hat{X}_a)/\sqrt{2} \\ \hat{Y}_u = (\hat{Y}_{in} + \hat{Y}_a)/\sqrt{2} \end{cases}, \quad (3)$$

where  $\hat{X}_{in}$ ,  $\hat{Y}_{in}$  represents amplitude and phase quadratures of the input state.

Alice sends another beam of EPR-entangled beams (mode  $b$ ) to Bob through a fiber channel (quantum channel). The distributed beams (mode  $b'$ ) is received by Bob at the terminal. We considered the fiber channel is a noise channel, which is close to a realistic fiber environment. When the optical mode transmitted over a noisy fiber channel, there are the vacuum noise and excess noise induced by the effect of the depolarized GAWBS in the fiber. The fluctuation of amplitude and phase quadratures of the distributed mode  $b$  over a noisy fiber channel can be given by [23]

$$\begin{cases} \delta \hat{X}_{b'} = \sqrt{\eta_b} \delta \hat{X}_b + \sqrt{1 - \eta_b} \delta \hat{X}_G + \sqrt{1 - \eta_b} \delta \hat{X}_{V_b} \\ \delta \hat{Y}_{b'} = \sqrt{\eta_b} \delta \hat{Y}_b + \sqrt{1 - \eta_b} \delta \hat{Y}_G + \sqrt{1 - \eta_b} \delta \hat{Y}_{V_b} \end{cases}, \quad (4)$$

where  $\delta \hat{X}_{b'}$ ,  $\delta \hat{Y}_{b'}$  are fluctuations of amplitude and phase quadratures of the beam  $b'$ .  $\delta \hat{X}_G$ ,  $\delta \hat{Y}_G$  and  $\delta \hat{X}_{V_b}$ ,  $\delta \hat{Y}_{V_b}$  represent fluctuations of amplitude and phase quadratures of the depolarized

GAWBS field and the vacuum field in the noisy fiber channel, respectively.  $\eta_b$  is the transmission efficiency of the fiber channel.  $\eta_b = \xi \times 10^{-\alpha L/10}$ ,  $\xi$  is the fiber coupler efficiency,  $L$  is the length of the fiber,  $\alpha$  is the loss coefficient of the fiber, which is typically 0.2 dB/km at 1550 nm.

Meanwhile, Alice encodes the classical information of the joint measurement to a synchronization beam based on optical modulated method. The balance homodyne detections (BHDs) are used to measure the amplitude and phase quadratures of the output mode from the BS. The normalized photocurrents from the photodetectors are given by  $\hat{i}_{1x}^-(t) = \hat{X}_u(t)$  and  $\hat{i}_{1y}^-(t) = \hat{Y}_u(t)$ , respectively. The photocurrents acted as the classical information are loaded on a synchronization beam through an amplitude and phase modulator. The encoded synchronization beam can be given by

$$\hat{s} = \hat{s}_0(1 + m\hat{i}_{1x}^- + im\hat{i}_{1y}^-), \quad (5)$$

where  $\hat{s}_0$  is the operator of the synchronization beam,  $m$  is the modulation depth of the modulators loaded on the synchronization beam. The amplitude and phase quadratures of the encoded synchronization beam can be written as

$$\begin{cases} \hat{X}_s = \hat{X}_{s_0} + 2mE\hat{X}_u \\ \hat{Y}_s = \hat{Y}_{s_0} - 2mE\hat{Y}_u \end{cases}. \quad (6)$$

where  $E$  is the mean field of the synchronization beam.  $\hat{X}_{s_0}$  and  $\hat{Y}_{s_0}$  is the amplitude and phase quadratures of the synchronization beam, respectively. The encoded synchronization beam is sent to Bob through a fiber channel (classical channel). The quantum and classical information are distributed synchronously over a same optical fiber. Bob decodes the classical information from the encoded synchronization beam. The amplitude and phase quadratures of the encoded synchronization beam in Bob's site are decoded by using the BHDs. The normalized photocurrents output from the BHDs can be written as

$$\begin{cases} \hat{i}_{2x}^- = 2\sqrt{\eta}mE\hat{X}_u + \sqrt{\eta}\hat{X}_{s_0} + \sqrt{1-\eta}\hat{X}_v - \hat{X}_{vB} \\ \hat{i}_{2y}^- = -2\sqrt{\eta}mE\hat{Y}_u + \sqrt{\eta}\hat{Y}_{s_0} + \sqrt{1-\eta}\hat{Y}_v + \hat{Y}_{vB} \end{cases}, \quad (7)$$

where  $\hat{X}_v$ ,  $\hat{Y}_v$  and  $\hat{X}_{vB}$ ,  $\hat{Y}_{vB}$  represent the amplitude and phase quadratures of the vacuum field in the fiber channel and 50/50 BS, respectively.  $\eta$  is the transmission efficiency of the fiber channel. By the Fourier transformation, the fluctuation variances of the photocurrents spectra output from the BHDs can be deduced as

$$\begin{cases} \langle \delta^2 \hat{i}_{2x}^- (\Omega) \rangle = 2\eta|E|^2 m^2 (\sigma_a + 1) + 4B \\ \langle \delta^2 \hat{i}_{2y}^- (\Omega) \rangle = 2\eta|E|^2 m^2 (\sigma_a + 1) + 4B \end{cases}, \quad (8)$$

where  $\Omega$  is the analysis frequency in the unit of hertz. The initial input state is a coherent state with the fluctuation variance of 1, i.e.  $\langle \delta \hat{X}_{in}^2 \rangle = \langle \delta \hat{Y}_{in}^2 \rangle = 1$ . The fluctuation variances of amplitude and phase quadratures of the output mode from the BS are  $\langle \delta^2 \hat{X}_u(\Omega) \rangle = \langle \delta^2 \hat{Y}_u(\Omega) \rangle = (\sigma_a + 1)/2$ , respectively. The fluctuation variances induced by the vacuum are equal to 1, i.e.  $\langle \delta^2 \hat{X}_v(\Omega) \rangle = \langle \delta^2 \hat{Y}_v(\Omega) \rangle = 1$  and  $\langle \delta^2 \hat{X}_{vB}(\Omega) \rangle = \langle \delta^2 \hat{Y}_{vB}(\Omega) \rangle = 1$ . The fluctuation variances of amplitude and phase quadratures of the synchronization beam is required to reach the shot noise limit (SNL) at the analysis frequency of  $\Omega$ , i. e.  $\langle \delta^2 \hat{X}_{s_0}(\Omega) \rangle = \langle \delta^2 \hat{Y}_{s_0}(\Omega) \rangle = 1$ . The mean photon number produced in unit time of the synchronization beam is  $|E|^2 = \lambda P_s / (hc)$ .  $P_s$  and  $\lambda$  is the power and wavelength of the synchronization beam, respectively.  $h$  is the Planck's constant and  $c$  is the velocity of light.  $B$  is the bandwidth of the BHDs.

The first and second items of the Eq. (8) represent the amplitude of the decoded classical information and the amplitude of the decoded noise, respectively. The first item can be increased

by increasing the power of the decoded synchronization beam and the modulation depth of the modulators loaded on the synchronization beam. So the influence of the decoded noise will be ignored, which is far less than the first item. Then the decoded classical information measured by the BHDs is normalized approximately:  $\delta\hat{i}_{2x}' = \delta\hat{X}_u$  and  $\delta\hat{i}_{2y}' = \delta\hat{Y}_u$ , which is the same as the classical information at Alice's site. It means that the synchronization of signals of the classical channel and quantum channel is realized. Subsequently, Bob implements unitary operation by loading the classical information on a translation beam in real time. The teleported state of the initial input state is obtained by coupling the translation beam with the distributed beam of EPR-entangled beams. The initial input state is retrieved by Bob, and a real time deterministic remote quantum teleportation is realized.

Fluctuations of amplitude and phase quadratures of the teleported state are

$$\begin{cases} \delta\hat{X}_{out} = \delta\hat{X}_{b'} + \sqrt{2}g_x\delta\hat{X}_u \\ \delta\hat{Y}_{out} = \delta\hat{Y}_{b'} + \sqrt{2}g_y\delta\hat{Y}_u \end{cases}, \quad (9)$$

where  $g$  is the gain factor of the classical channel, which usually has an equivalent value for amplitude ( $g_x$ ) and phase ( $g_y$ ) quadratures because the two quadrature components are symmetric. If  $g$  is selected to be unity, arbitrary quantum states can be transferred with the presented system [13,16,24]. Thus,  $g_x = g_y = 1$  is considered here.

In the single-channel scheme, an obvious advantage is that the beam  $a$  retained in Alice's station can be manipulated to achieve optimal quantum teleportation with high fidelity and long transmission distance. A lossy channel is established for the beam  $a$ , and the transmission efficiency ( $\eta_a$ ) for the beam  $a$  can continuously adjusted and optimized. The amplitude and phase quadratures of the mode  $a$  can be rewritten as  $\hat{X}_{a'} = \sqrt{\eta_a}\hat{X}_a + \sqrt{1-\eta_a}\hat{X}_{V_a}$  and  $\hat{Y}_{a'} = \sqrt{\eta_a}\hat{Y}_a + \sqrt{1-\eta_a}\hat{Y}_{V_a}$ , where  $\hat{X}_{V_a}$  and  $\hat{Y}_{V_a}$  represent the amplitude and phase quadratures of the vacuum, respectively. Equation (9) can be deduced as

$$\begin{cases} \delta\hat{X}_{out} = \sqrt{\eta_b}\delta\hat{X}_b + \sqrt{1-\eta_b}\delta\hat{X}_G + \sqrt{1-\eta_b}\delta\hat{X}_{V_b} + \delta\hat{X}_{in} - \sqrt{\eta_a}\delta\hat{X}_a - \sqrt{1-\eta_a}\delta\hat{X}_{V_a} \\ \delta\hat{Y}_{out} = \sqrt{\eta_b}\delta\hat{Y}_b + \sqrt{1-\eta_b}\delta\hat{Y}_G + \sqrt{1-\eta_b}\delta\hat{Y}_{V_b} + \delta\hat{Y}_{in} + \sqrt{\eta_a}\delta\hat{Y}_a + \sqrt{1-\eta_a}\delta\hat{Y}_{V_a} \end{cases}. \quad (10)$$

Therefore, fluctuation variances of amplitude and phase quadratures of the teleported state can be expressed as

$$\begin{cases} \langle \delta\hat{X}_{out}^2 \rangle = \eta_b \langle \delta\hat{X}_b^2 \rangle + \eta_a \langle \delta\hat{X}_a^2 \rangle - 2\sqrt{\eta_b\eta_a} \langle \delta\hat{X}_a\delta\hat{X}_b \rangle + (1-\eta_b) \langle \delta\hat{X}_G^2 \rangle \\ \quad + (1-\eta_b) \langle \delta\hat{X}_{V_b}^2 \rangle + (1-\eta_a) \langle \delta\hat{X}_{V_a}^2 \rangle + \langle \delta\hat{X}_{in}^2 \rangle \\ \langle \delta\hat{Y}_{out}^2 \rangle = \eta_b \langle \delta\hat{Y}_b^2 \rangle + \eta_a \langle \delta\hat{Y}_a^2 \rangle + 2\sqrt{\eta_b\eta_a} \langle \delta\hat{Y}_a\delta\hat{Y}_b \rangle + (1-\eta_b) \langle \delta\hat{Y}_G^2 \rangle \\ \quad + (1-\eta_b) \langle \delta\hat{Y}_{V_b}^2 \rangle + (1-\eta_a) \langle \delta\hat{Y}_{V_a}^2 \rangle + \langle \delta\hat{Y}_{in}^2 \rangle \end{cases}. \quad (11)$$

The fluctuation variances induced by the vacuum is equal to 1, i.e.  $\langle \delta\hat{X}_{V_a}^2 \rangle = \langle \delta\hat{Y}_{V_a}^2 \rangle = 1$  and  $\langle \delta\hat{X}_{V_b}^2 \rangle = \langle \delta\hat{Y}_{V_b}^2 \rangle = 1$ . The variance of the extra noise induced by the depolarized GAWBS can be written as  $\langle \delta\hat{X}_G^2 \rangle = \langle \delta\hat{Y}_G^2 \rangle = \eta_b P_{LO} \varepsilon L$ ,  $P_{LO}$  is the power of the local oscillator (LO) distributed together in the fiber channel with the beam  $b$ ,  $\varepsilon$  is the photon scattering efficiency of the fiber due to the effect of the depolarized GAWBS [26]. We define  $\sigma_x = \langle \delta\hat{X}_{out}^2 \rangle$ ,  $\sigma_y = \langle \delta\hat{Y}_{out}^2 \rangle$ . The fluctuation variances of amplitude and phase quadratures of the teleported state are considered

be identical. Equation (11) can be deduced as

$$\sigma_x = \sigma_y = \eta_b(\sigma_b - 1) + \eta_a(\sigma_a - 1) - 2\sqrt{\eta_a\eta_b}\sigma_{ab} + (1 - \eta_b)\eta_b P_{LO}\varepsilon L + 3. \quad (12)$$

The fidelity is a physical quantity that aids in quantifying the quality of quantum teleportation. It is expressed as [13]

$$F = 2/\sqrt{(1 + \sigma_x)(1 + \sigma_y)}. \quad (13)$$

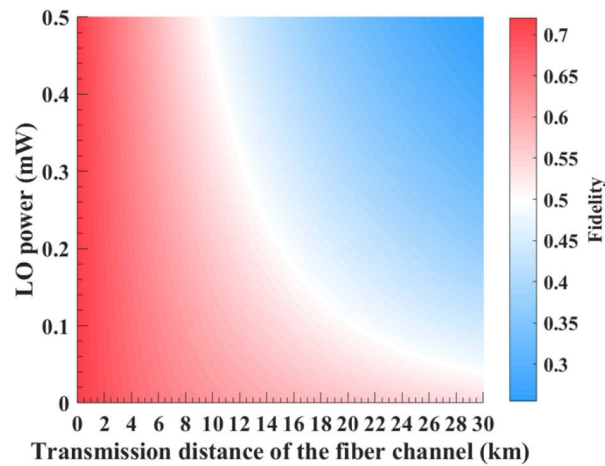
Substituting Eq. (12) into Eq. (13), the fidelity of the deterministic quantum teleportation based on the single-fiber-channel scheme can be obtained as

$$F = \frac{2}{4 + \eta_b(\sigma_b - 1) + \eta_a(\sigma_a - 1) - 2\sqrt{\eta_a\eta_b}\sigma_{ab} + (1 - \eta_b)\eta_b P_{LO}\varepsilon L}. \quad (14)$$

It can be seen that the fidelity of the deterministic quantum teleportation based on the single-fiber-channel scheme depends on the quality of the EPR quantum entangled state, the transmission efficiency and the extra noise of the fiber channel, and the transmission efficiency of the lossy channel for the beam  $a$ . According to Eq. (14), the maximum fidelity can be obtained by taking the minimum value of  $\sigma_x$  and  $\sigma_y$  ( $\sigma_x = \sigma_y$ ), that is  $d\sigma_{x(y)}/d\eta_a = 0$ . Consequently, when  $\eta_a = \left(\frac{\sigma_{ab}}{\sigma_a - 1}\right)^2 \eta_b$ , the maximum fidelity can be obtained. It can be seen that the optimal transmission efficiency of  $\eta_a$  depends not only on the quality of the EPR entangled state, but also on the transmission distance of the optical fiber.

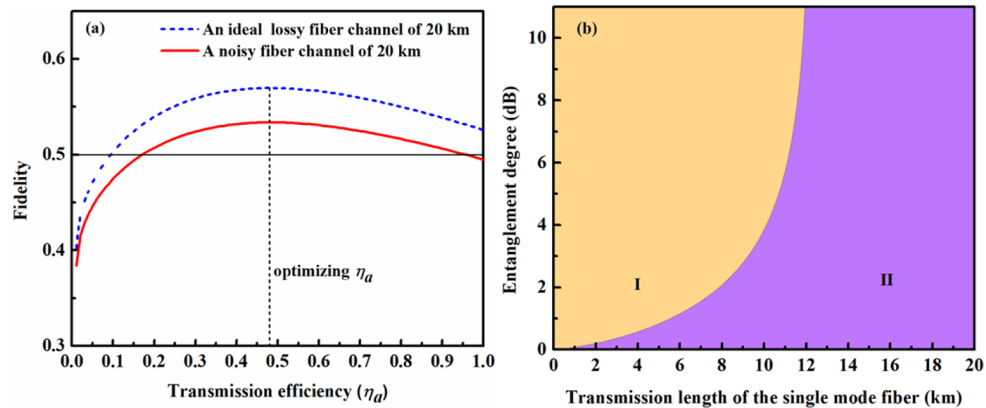
Figure 1 shows the theoretically calculated fidelity of the deterministic quantum teleportation based on the single-fiber-channel scheme as functions of the transmission distance of the fiber channel and the power of the LO using Eq. (14). In the theoretical calculation,  $\sigma_a = 4.09$ ,  $\sigma_b = 4.01$  and  $\sigma_{ab} = 3.73$  when the entanglement degree of EPR-entangled beams is set to 5 dB which is consistent with our current experiment,  $\xi = 0.81$  and  $\varepsilon = 0.35 \text{ W}^{-1}\text{m}^{-1}$ .  $\eta_a$  is optimized for different transmission distances of the fiber channel. It can be seen that the fidelity of quantum teleportation will decrease with the increase of the transmission distance and LO power. Obviously, the influence of the LO power on the fidelity is small when the transmission distance of the fiber channel is short, and the influence of the LO power on the fidelity becomes more serious with the increase of the transmission distance. For instance, when the LO power in the fiber is zero, the fiber is equivalent to an ideal lossy fiber channel in which only vacuum noise is existed. In the case, the fidelity of quantum teleportation is always higher than the classical limit of 1/2. When the LO power in the fiber is 0.2 mW, the fidelity of quantum teleportation is still higher than the classical limit of 1/2 when the transmission distance is 15 km. If the transmission distance increases to 30 km, the fidelity of quantum teleportation is smaller than the classical limit of 1/2 unless the LO power in the fiber is lower than 0.1 mW. The higher quality BHD with the high-gain and low-noise need to be developed in the case of such lower LO power.

Figure 2(a) shows the theoretically calculated fidelity of the deterministic quantum teleportation based on the single-fiber-channel scheme as functions of the transmission efficiency of the lossy channel for the beam  $a$ . The blue dashed line and red solid line are the fidelity along with the transmission efficiency of  $\eta_a$  over the ideal lossy fiber and noisy fiber, respectively. A fixed transmission distance of 20 km fiber channel was given, and the entanglement degree of EPR-entangled beams was set to be 5 dB. It can be seen that the fidelity of the deterministic quantum teleportation based on the single-fiber-channel scheme can be improved by optimizing the transmission efficiency of the lossy channel for the beam  $a$ . When  $\eta_a$  is optimized to 0.47, the fidelity of quantum teleportation over the ideal lossy fiber and noisy fiber can reach the maximum values of 0.57 and 0.53, respectively. When the loss of the lossy channel is 0, that is  $\eta_a = 1$ , the fidelity over the ideal lossy fiber and noisy fiber are 0.52 and 0.49, respectively. The transmission efficiency of  $\eta_a$  is not as bigger as better. The optimizing  $\eta_a$  will be changed



**Fig. 1.** Fidelity of deterministic quantum teleportation versus the LO power and transmission distance of the fiber channel.

with different transmission distances. The entanglement versus the transmission distance of the deterministic quantum teleportation based over the noisy fiber channel is discussed, as shown in Fig. 2(b). Region I represent the deterministic quantum teleportation can be realized. Region II represent the fidelity of quantum teleportation is less than the classical limit of  $1/2$  and quantum teleportation cannot be realized. The maximum transmission distance of the deterministic quantum teleportation is 10.7 km with a 5 dB EPR-entangled beams that is consistent with our current experiment. The power of the LO is set to be 0.4 mW, which is the minimum power to meet the requirements of the experimental requirements at present. The transmission distance is no significant increase when the entanglement degree of EPR-entangled beams increases. So far, when the EPR-entangled beams with the entanglement degree of 11 dB was used, the maximum transmission distance of the deterministic quantum teleportation is 12.2 km. It means that the higher degree entangled state is more sensitive to the losses of fiber channel.



**Fig. 2.** (a). Fidelity of deterministic quantum teleportation versus the transmission efficiency of the lossy channel established at Alice's site. (b). Fidelity of deterministic quantum teleportation versus the entanglement degree of EPR entangled states.

### 3. Experimental setup

The experimental scheme for real time deterministic quantum teleportation over a single fiber channel is shown in Fig. 3. The generation of the EPR-entangled beams at telecommunication wavelength of 1550 nm had been described in detail in Ref. [27]. When NOPA was subthreshold operated in the state of amplification, EPR-entangled beams with correlated amplitude quadratures and anti-correlated phase quadratures were generated. The prepared EPR-entangled beams which have the identical frequency and orthogonal polarization were divided into two beams (a and b) through a polarizing beam splitter (PBS).

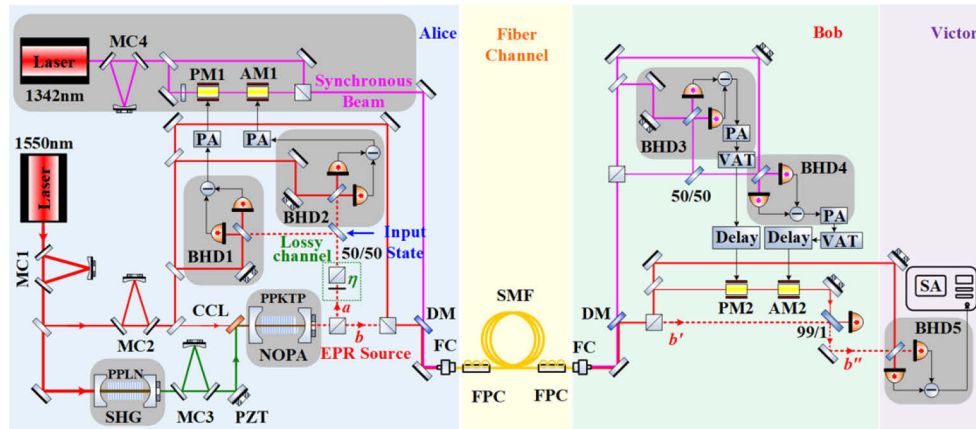


**Fig. 3.** Experimental scheme for real time deterministic quantum teleportation over a single fiber channel. MC1-2: mode cleaner of 1550 nm; SHG: second harmonic generator; MC3: mode cleaner of 775 nm; MC4: mode cleaner of 1342 nm; PZT: piezo-electric transducer; NOPA: nondegenerate optical parametric amplifier; PM: phase modulator; AM: amplitude modulator; PA: power amplifier; FC: fiber coupler; FPC: fiber polarization controllers; SMF: single mode fiber; VAT: variable attenuator; BHD1-5: balance homodyne detector; SA: spectrum analyser.

The sender (Alice) in the local site reserved the beam  $a$  and sent the beam  $b$  to receiver (Bob) through a fiber channel (quantum channel). The beam  $b$  and LO at 1550 nm were coupled by polarization multiplexing and distributed to the remote Bob over a SMF. This method can avoid relative phase jitter of two beams in two SMFs. Alice combined the beam  $a$  and an input coherent state, which was going to be teleported, on a 50/50 BS and made a joint measurement using BHD1 and BHD2. The classical information of joint measurement results was amplified by power amplifiers (PA) and encoded to a 1342 nm laser beam in Alice's site using the amplitude modulator (AM1) and the phase modulator (PM1), respectively. Signal to noise ratios of the modulated signals can be improved by increasing the gain of PAs and LO powers of BHD1 and BHD2. The encoded 1342 nm laser was used to transfer the classical information of joint measurement in real time to remote Bob through the same SMF (classical channel). The encoded 1342 nm beam and LO at 1342 nm was coupled into the same SMF by polarization multiplexing and distributed together with the beam  $b$  and LO at 1550 nm to Bob. A dichroic mirror (DM,  $R_{1550\text{ nm}} > 99.9\%$  &  $R_{1342\text{ nm}} < 0.1\%$ ) was using to couple beams at 1550 nm and 1342 nm into the fiber coupler (FC). The fiber polarization controllers (FPCs) were employed to maintain the same polarization of the beams. Meanwhile, the 1342 nm beam also acted as a synchronous beam to realize the synchronization of the quantum and classical information, which were distributed synchronously over the same SMF. The wavelength of the synchronous beam at 1342 nm and that of the distributed signal beam at 1550 nm was difference that can eliminate the cross-talk in

the fiber channel. A fixed time delay was used to compensate for the velocity difference between 1550 nm and 1342 nm beam in the SMF.

At the terminal of the SMF channel, beams at 1550 nm and at 1342 nm were separated by DM. The beam  $b'$  and LO at 1550 nm, as well as the encoded 1342 nm synchronous beam and LO at 1342 nm, were polarization demultiplexed. Bob decoded the classical information from the encoded 1342 nm synchronization beam using BHD3 and BHD4. The decoded classical information was amplified by PAs, amplitude adjusted by variable attenuators (VAT), time delayed by delay boxes, and loaded on a translation beam using the AM2 and PM2. The translation beam was a small part beam of the transmitted LO at 1550 nm. The corresponding unitary operation was performed by coupling the beam  $b'$  with the translation beam using one 1/99 BS in real time. The relative phase between the beam  $b'$  and translation beam was locked using a coherent control light (CCL) by the coherent control technology [28]. Meanwhile, the relative phases between measured beams and corresponding LOs injected to BHD1, BHD 2, BHD 3, and BHD 4 were also locked using CCLs. The teleported state (beam  $b''$ ) was obtained at Bob's site. It means, the input state destroyed by the joint measurements at Alice's site was recovered at Bob's site under the help of nonlocal quantum entanglement.

In deterministic quantum teleportation scheme over the single fiber channel, a lossy channel formed by a half wave plate (HWP) and a PBS was established to manipulate the beam  $a$  of EPR-entangled beams at Alice's site. The fidelity and the transmission distance of the fiber were studied when the transmission efficiency of the lossy channel was adjusted. Bob sent the teleported output state and LO at 1550 nm into the inspection station (Victor). Victor made a verification measurement using BHD5. The fidelity for deterministic quantum teleportation was estimated by measurement results from Victor.

#### 4. Experimental results and discussion

The noise powers of the EPR-entangled beams generated by the NOPA were measured firstly. The measured threshold of the NOPA was 46 mW. When the pump power was 40 mW and the relative phase between the pump and injected CCL was locked to 0, EPR-entangled beams with correlated amplitude quadratures and anticorrelated phase quadratures were generated. Noise powers of NOPA output beams were measured using BHD and recorded by a spectrum analysis (SA), as shown in Fig. 4. The curve (i) is the SNL. The curves (ii) is the electronics noise level (ENL) that is 13 dB below the SNL, the influence of the ENL can be ignored. The curves (iii) and (iv) are measured noise powers of the amplitude difference and phase sum of NOPA output beams, respectively. It can be seen that noise powers are 5.08 dB and 4.96 dB below the SNL, respectively. The curves (v) and (vi) are the measured noise powers of quadrature amplitudes of the beam  $a$  and  $b$ , respectively. It can be seen that noise powers are 6.12 dB and 6.03 dB higher than the SNL. The measured noise powers of quadrature phases of the beam  $a$  and  $b$  were identical with that of quadrature amplitudes. The parameters of SA were as follows: Fourier analysis frequency was 2.5 MHz in the zero-span mode, resolution bandwidth (RBW) was 100 kHz, video bandwidth (VBW) was 100 Hz, and the sweep time was 500 ms. Using the measured data, the covariance matrix of measured EPR-entangled beams can be written as

$$\sigma = \begin{pmatrix} 4.09 & 0 & 3.74 & 0 \\ 0 & 4.09 & 0 & -3.73 \\ 3.74 & 0 & 4.01 & 0 \\ 0 & -3.73 & 0 & 4.01 \end{pmatrix}. \quad (15)$$

Generally, a classical teleportation needs to be implemented firstly by blocking the EPR-entangled beams to calibrate the gain of the classical channel. In this crucial step, the measured

noise power of the output beam  $b''$  was 4.8 dB higher than the SNL through carefully adjusting VATs. It means that the gain factors of the classical channel in our experiment can be treat as unity for simplicity [14]. Then, the EPR-entangled beams were exploited to realize the quantum teleportation. In order to reduce the extra noise induced by the depolarized GAWBS in the fiber, the power of the LO and translation beam at 1550 nm at Bob's site were 0.2 mW, respectively, which is the lowest power for the BHD system and translation operating. The relative phases between measured beams and corresponding LOs injected to BHD1, BHD 2, BHD 3, and BHD 4 were locked to  $0, \pi/2, \pi/2, 0$ , respectively. The relative phase between the beam  $b'$  and translation beam was locked to 0. After the quantum teleported state was obtained at Bob's site under the help of quantum entanglement, the value of the fidelity for deterministic quantum teleportation was estimated by measurement results from Victor using Eq. (13).

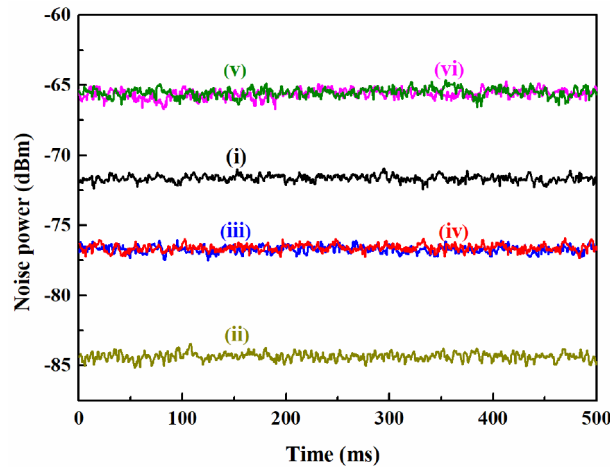


**Fig. 4.** Noise powers of NOPA output beams. curve (i) is the SNL; curve (ii) is the ENL; curves (iii) and (iv) are measured noise powers of the amplitude difference and phase sum of the beam  $a$  and  $b$ , respectively; curve (v) and (vi) are the noise power of quadrature amplitudes of the beam  $a$  and  $b$ , respectively. The parameters of SA: RBW is 100 kHz and VBW is 100 Hz.

The fidelity of the deterministic quantum teleportation as a function of the transmission distance of the fiber channel is shown in Fig. 5. The dots with the error bar in Fig. 5 are experimental results. The blue diamonds are experimental data without optimizing  $\eta_a$  at Alice's site. It can be seen, when the transmission distance of the fiber channel is 7.0 km, the fidelity of the deterministic quantum teleportation is  $0.52 \pm 0.01$ , which is higher than the classical teleportation limit of  $1/2$ . When the transmission distance is 10.0 km, the fidelity decreases to  $0.46 \pm 0.01$  that is smaller than the classical teleportation limit of  $1/2$ . The red circles are experimental data with optimizing  $\eta_a$  at Alice's site. When the transmission distance is 10.0 km, the fidelity of the deterministic quantum teleportation is  $0.51 \pm 0.01$ , which is higher than the classical teleportation limit of  $1/2$ . It means that the real time deterministic quantum teleportation over 10 km of optical fiber was realized experimentally. Moreover, the fidelity is  $0.67 \pm 0.01$ , which is higher than the no-cloning limit of  $2/3$ , when the transmission distance of the fiber channel is 2 km. The red and blue dashed line in Fig. 5 is the theoretically predicted fidelity over the ideal lossy fiber channel with and without optimizing  $\eta_a$  using Eq. (14), respectively. The fidelity is higher than the classical teleportation limit of  $1/2$  when the transmission distance is up to 20 km. Clearly, the theoretically predictions have large discrepancies with experimental results if the excess noise induced by the effect of the depolarized GAWBS in the fiber is not considered. The red and blue solid lines in Fig. 4 are the theoretically predicted fidelity over the noisy fiber channel

with and without optimizing  $\eta_a$  using Eq. (14), respectively. The parameters in the theoretical predictions are as follows: the covariance matrix elements of the initial EPR-entangled beams are given in Eq. (15), the power of the distributed LO at Alice's site is  $0.4/\eta_b$  mW, the value of  $\xi$  and  $\varepsilon$  is mentioned in the second section. It can be seen that theoretical predictions are in good agreement with experimental results. Obviously, the fidelity can be improved through manipulating beam  $a$  of EPR-entangled beams in Alice's site, and the improvement is greater along with longer transmission distance of the fiber channel. The maximum transmission distance of the deterministic quantum teleportation can be reach to 10.7 km when  $\eta_a$  is optimized.

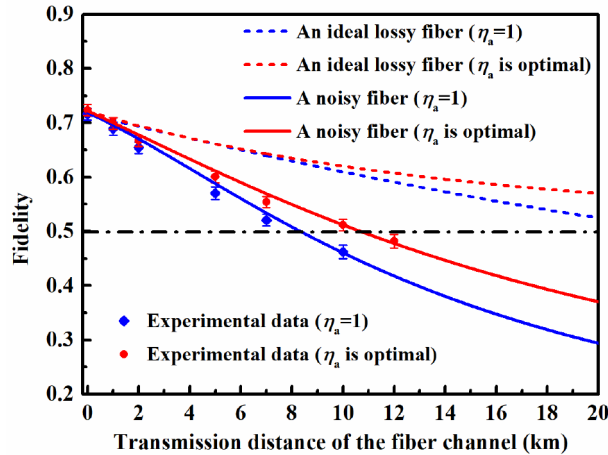


**Fig. 5.** Fidelity of the deterministic quantum teleportation versus the transmission distance of the fiber channel.

The fidelity and transmission distance of the deterministic quantum teleportation are mainly limited by the entanglement degree of EPR-entangled beams in the current experimental system. If the entanglement degree of EPR-entangled beams is reached 10 dB, the calculated transmission distance of the fiber channel for the deterministic quantum teleportation can be more than 20 km. In addition, the extra noise induced by the effect of the depolarized GAWBS in the fiber channel is another influence factor on the deterministic quantum teleportation. The influence of the extra noise can be reduced by decreasing the LO power in the fiber channel, but the higher gain and lower noise BHD system needs to be developed to detect weaker signals.

## 5. Conclusion

A deterministic quantum teleportation based on a single-fiber-channel scheme was designed. A lossy channel was established to manipulate the beam of EPR entanglement in Alice's station. The dependences of the fidelity on the transmission distance of the fiber channel, excess noise induced by the effect of the depolarized GAWBS in the fiber and the transmission efficiency of the lossy channel were theoretically analyzed. The fidelity of quantum teleportation will decrease with the increase of the transmission distance and LO power, and the transmission distance of the deterministic quantum teleportation can be increased by optimizing the transmission efficiency of the lossy channel. Based on the theoretical analysis, a real time deterministic quantum teleportation over a single fiber channel was implemented experimentally by exploiting the EPR entanglement at 1550 nm. The EPR entangled beams (beam  $a$  and  $b$ ) at 1550 nm were generated experimentally from a single NOPA firstly, the measured correlation variance of the amplitude difference and phase sum of the EPR entangled beams were 5.08 dB and 4.96 dB below the SNL, respectively. A 1342 nm laser beam was used to transfer the classical information in real time

and also acted as a synchronous beam to realize the synchronization of the quantum and classical information. The quantum and classical information were distributed synchronously over a same SMF. A real time deterministic remote quantum teleportation was realized. The dependence of the fidelity on the transmission distance of the fiber channel was studied experimentally with and without optimizing the transmission efficiency of the lossy channel. The maximum transmission distance of the deterministic quantum teleportation can be reach to 10 km with the fidelity of  $0.51 \pm 0.01$ , which is higher than the classical teleportation limit of  $1/2$ . The fidelity was higher than the no-cloning limit of  $2/3$  when the transmission distance of the fiber channel was 2 km. The transmission distance of 10 km for the deterministic quantum teleportation over fiber channel is sufficient for constructing a metropolitan quantum network. The work provides a feasible scheme to establish metropolitan quantum networks over fiber channels based on deterministic quantum teleportation.

**Funding.** National Natural Science Foundation of China (62175135).

**Disclosures.** The authors declare no conflicts of interest.

**Data availability.** Data underlying the results presented in this paper are not publicly available at this time but can be obtained from the authors upon reasonable request.

## References

1. S. Pirandola, J. Eisert, C. Weedbrook, A. Furusawa, and S. L. Braunstein, "Advances in quantum teleportation," *Nat. Photonics* **9**(10), 641–652 (2015).
2. C. Weedbrook, S. Pirandola, R. G. Patrón, N. J. Cerf, T. C. Ralph, J. H. Shapiro, and S. Lloyd, "Gaussian quantum information," *Rev. Mod. Phys.* **84**(2), 621–669 (2012).
3. S. L. Braunstein and P. V. Loock, "Quantum information with continuous variables," *Rev. Mod. Phys.* **77**(2), 513–577 (2005).
4. A. Einstein, B. Podolsky, and N. Rosen, "Can quantum mechanical description of physical reality be considered complete?" *Phys. Rev.* **47**(10), 777–780 (1935).
5. Z. Y. Ou, S. F. Pereira, H. J. Kimble, and K. C. Peng, "Realization of the Einstein-Podolsky-Rosen paradox for continuous variables," *Phys. Rev. Lett.* **68**(25), 3663–3666 (1992).
6. W. H. Zhang, N. J. Jiao, R. X. Li, L. Tian, Y. J. Wang, and Y. H. Zheng, "Precise control of squeezing angle to generate 11 dB entangled state," *Opt. Express* **29**(15), 24315–24325 (2021).
7. C. H. Bennett, G. Brassard, C. Crepeau, R. Jozsa, A. Peres, and W. K. Wootters, "Teleporting an unknown quantum state via dual classical and Einstein-Podolsky-Rosen channels," *Phys. Rev. Lett.* **70**(13), 1895–1899 (1993).
8. D. Bouwmeester, J. W. Pan, K. Mattle, M. Eibl, H. Weinfurter, and A. Zeilinger, "Experimental quantum teleportation," *Nature* **390**(6660), 575–579 (1997).
9. X. S. Ma, T. Herbst, T. Scheidl, D. Wang, S. Kropatschek, W. Naylor, B. Wittmann, A. Mech, J. Kofler, E. Anisimova, V. Makarov, T. Jennewein, R. Ursin, and A. Zeilinger, "Quantum teleportation over 143 kilometres using active feed-forward," *Nature* **489**(7415), 269–273 (2012).
10. J. G. Ren, P. Xu, H. L. Yong, L. Zhang, S. K. Liao, J. Yin, W. Y. Liu, W. Q. Cai, M. Yang, L. Li, K. X. Yang, X. Han, Y. Q. Yao, J. Li, H. Y. Wu, S. Wan, L. Liu, D. Q. Liu, Y. W. Kuang, Z. P. He, P. Shang, C. Guo, R. H. Zheng, K. Tian, Z. C. Zhu, N. L. Liu, C. Y. Lu, R. Shu, Y. A. Chen, C. Z. Peng, J. Y. Wang, and J. W. Pan, "Ground-to-satellite quantum teleportation," *Nature* **549**(7670), 70–73 (2017).
11. I. Marcikic, H. de Riedmatten, W. Tittel, H. Zbinden, and N. Gisin, "Long-distance teleportation of qubits at telecommunication wavelengths," *Nature* **421**(6922), 509–513 (2003).
12. H. Takesue, S. D. Dyer, M. J. Stevens, V. Verma, R. P. Mirin, and S. W. Nam, "Quantum teleportation over 100 km of fiber using highly efficient superconducting nanowire single-photon detectors," *Optica* **2**(10), 832–835 (2015).
13. A. Furusawa, J. L. Sørensen, S. L. Braunstein, C. A. Fuchs, H. J. Kimble, and E. S. Polzik, "Unconditional quantum teleportation," *Science* **282**(5389), 706–709 (1998).
14. T. C. Zhang, K. W. Goh, C. W. Chou, P. Lodahl, and H. J. Kimble, "Quantum teleportation of light beams," *Phys. Rev. A* **67**(3), 033802 (2003).
15. X. J. Jia, X. L. Su, Q. Pan, J. R. Gao, C. D. Xie, and K. C. Peng, "Experimental demonstration of unconditional entanglement swapping for continuous variables," *Phys. Rev. Lett.* **93**(25), 250503 (2004).
16. N. Takei, H. Yonezawa, T. Aoki, and A. Furusawa, "High-fidelity teleportation beyond the no-cloning limit and entanglement swapping for continuous variables," *Phys. Rev. Lett.* **94**(22), 220502 (2005).
17. N. Lee, H. Benichi, Y. Takeda, S. Takeda, J. Webb, E. Huntington, and A. Furusawa, "Teleportation of nonclassical wave packets of light," *Science* **332**(6027), 330–333 (2011).
18. J. F. Sherson, H. Krauter, R. K. Olsson, B. Julsgaard, K. Hammerer, I. Cirac, and E. S. Polzik, "Quantum teleportation between light and matter," *Nature* **443**(7111), 557–560 (2006).
19. Y. A. Chen, S. Chen, Z. S. Yuan, B. Zhao, C. S. Chuu, J. Schmiedmayer, and J. W. Pan, "Memorybuiltin quantum teleportation with photonic and atomic qubits," *Nat. Phys.* **4**(2), 103–107 (2008).

20. H. Krauter, D. Salart, C. A. Muschik, J. M. Petersen, H. Shen, T. Fernholz, and E. S. Polzikl, "Deterministic quantum teleportation between distant atomic objects," *Nat. Phys.* **9**(7), 400–404 (2013).
21. W. B. Gao, P. Fallahi, E. Togan, A. Delteil, Y. S. Chin, J. Miguel-Sanchez, and A. Imamoglu, "Quantum teleportation from a propagating photon to a solid-state spin qubit," *Nat. Commun.* **4**(1), 2744 (2013).
22. F. Bussi eres, C. Clausen, A. Tiranov, B. Korzh, V. B. Verma, S. W. Nam, F. Marsili, A. Ferrier, P. Goldner, H. Herrmann, C. Silberhorn, W. Sohler, M. Afzelius, and N. Gisin, "Quantum teleportation from a telecom-wavelength photon to a solid-state quantum memory," *Nat. Photonics* **8**(10), 775–778 (2014).
23. J. X. Feng, Z. J. Wan, Y. J. Li, and K. S. Zhang, "Distribution of continuous variable quantum entanglement at a telecommunication wavelength over 20 km of optical fiber," *Opt. Lett.* **42**(17), 3399–3402 (2017).
24. M. R. Huo, J. L. Qin, J. L. Cheng, Z. H. Yan, Z. Z. Qin, X. L. Su, X. J. Jia, C. D. Xie, and K. C. Peng, "Deterministic quantum teleportation through fiber-channels," *Sci. Adv.* **4**(10), eaas9401 (2018).
25. F. A. S. Barbosa, A. J. de Faria, A. S. Coelho, K. N. Cassemiro, A. S. Villar, P. Nussenzweig, and M. Martinelli, "Disentanglement in bipartite continuous-variable systems," *Phys. Rev. A* **84**(5), 052330 (2011).
26. R. M. Shelby, M. D. Levenson, and P. W. Bayer, "Guided acoustic-wave Brillouin scattering," *Phys. Rev. B* **31**(8), 5244–5252 (1985).
27. J. X. Feng, Z. J. Wan, Y. J. Li, and K. S. Zhang, "Generation of 8.3 dB continuous variable quantum entanglement at a telecommunication wavelength of 1550 nm," *Laser Phys. Lett.* **15**(1), 015209 (2018).
28. H. Vahlbruch, S. Chelkowski, B. Hage, A. Franzen, K. Danzmann, and R. Schnabel, "Coherent control of vacuum squeezing in the gravitational-wave detection band," *Phys. Rev. Lett.* **97**(1), 011101 (2006).